*Pure & Appl. Chem.*, Vol. 62, No. 9, pp. 1675–1680, 1990.
Printed in Great Britain.


# Effects of chemical reactions in arcs

Heinz H. Maecker

Technical University of Munich, Fed. Rep. of Germany

Abstract - In constricted arcs temperatures of almost 30 000 K can be produced. In the temperature gradients chemical reactions like dissociations and ionizations occur steadily. The changing composition of the arc plasma with temperature is the basis of valuable spectroscopic diagnostic methods. Furthermore the diffusion processes in reaction zones transporting the high reaction energy outwards contribute considerably to the heat conduction and influence the performance of arcs in a typical way. Finally, mass separation in reaction zones occur such that the component being more difficultly to be dissociated or ionized is gathered at higher temperatures. Similarly the electric field drives trace elements to the cathode where they collect the more the lower the ionization energy is (cataphoresis).

## 1 THE ELECTRIC ARC

The electric arc is a gas discharge at atmospheric or elevated pressure with currents in the A to kA range. The plasma of the arc columns is close to the state of local thermodynamic equilibrium, i.e. population densities and chemical reactions are governed by the local temperature. The radiation field, however, does not correspond to the respective blackbody radiation. Arc plasmas are rather transparent in the visible and in the near ultraviolet spectral region. In every day life, arcs are encountered for example in sun lamps, in high pressure mercury or sodium lamps for road illumination, in welding processes on shipyards, etc. In contrast, low pressure gas discharge lamps make use of glow discharges with relatively high electron temperatures and low temperatures of the heavy particles. In electrical arcs, axis temperatures of 30 000 K or more can be achieved under stable and geometrically well defined conditions, provided the arcs are properly constricted. In this respect, the so-called cascade arc chamber (Fig.1) is a valuable tool for heating gases up to full dissociation and single or even double ionization. It consists of a stack of copper plates a few millimeters thick and insulated from each other by very thin spacers of few tenth of a millimeter. The copper plates have central holes of a few to several millimeters diameter which are alined to form a cylindrical tube in the centre of the stack. Each plate is internally cooled by an intense water flow directed radially towards the outer wall of the arc channel. With suitable electrodes at each end of the cascade, the arc burns in the central channel of the cascade chamber and can be observed either side-on through tiny slits between two neighbouring cascade plates or end-on by proper off-axis arrangement of the electrodes. Such cascade arc chambers allow almost 20 kW/cm power input per unit arc length and about 20 kW/cm$^2$ wall load. These arcs are steady and of complete cylindrical symmetry.

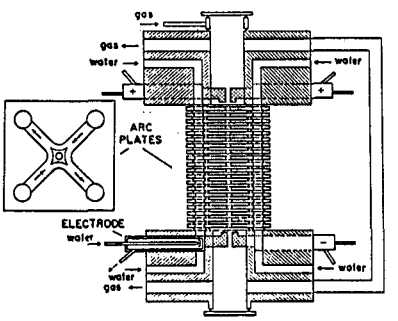


Fig. 1 Cascade arc chamber for heating gases up to almost 30 000 K /1/.

## 2 SPECTROSCOPIC DIAGNOSTICS, LARENZ MAXIMUM

The spectra of such wall-stabilized arcs (Fig. 2) consist not only of the bands of the molecules and the lines of the atoms but also of lines of singly and doubly charged ions. This allows the conclusion that the axis temperatures of the arc are in the range of about 25 000 K. Therefore we are interested in the composition of the arc gas for a high degree of dissociation and ionization. These chemical reactions are governed by the mass action law which, in case of binary dissociation, is given by

$$\frac{n_a^2}{n_m} = \frac{Z_a^2}{Z_m} \frac{(\pi m_a kT)^{3/2}}{h^3} e^{-E_D/kT} \qquad (1)$$

($n_a$, $n_n$ = number densities of atoms and molecules resp.; Z = partition function; $E_D$ = dissociation energy) and in case of the ionization by the Eggert-Saha-equation

$$\frac{n_{z+1}}{n_z} n_e = \frac{2\, Z_{z+1}}{Z_z} \frac{(2\pi m_e kT)^{3/2}}{h^3} e^{-E_I/kT} \qquad (2)$$

($n_e$, $n_z$, $n_{z+1}$ are the number densities of the electrons and the ions with the charge z, z+1 respectively, $E_I$=ionization energy. The other characters have the usual meaning). Regarding the pressure as

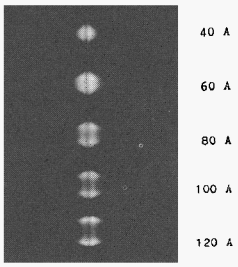


a)

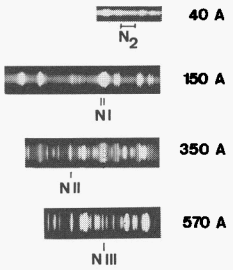


b)

Fig. 2 a) End-on spectrum of the hydrogen line $H_\beta$ at various currents /2/. Notice the Larenz maximum along the line and the broadening in $\lambda$-direction.
b) Side-on spectrum of the nitrogen arc at various currents /3/.

being constant in the arc, and assuming quasi-neutrality $\sum q_j n_j = 0$ all particle number densities can be calculated as functions of the temperature and the given pressure p (Fig.3). Whilst the total number density decreases inversely with temperature according to the general gas law n = p/kT the molecules dissappear more rapidly with increasing temperatures due to dissociation. In contrast, the atom and ion number densities first increase and then fall according to dissociation and ionization, respectively. Introducing the Boltzmann distribution over the excited states m of any species

$$\frac{n_m}{n} = \frac{g_m}{Z} e^{-E_m/kT} \tag{3}$$

and employing Einstein's transition probabilities $A_{mn}$ we obtain for the absolute intensity of a spectral line emitted from a homogenous layer of length $l$

$$I_L = \frac{h\nu_L}{4\pi} A_{mn} \cdot n \cdot e^{-E_m/kT} \cdot l \tag{4}$$

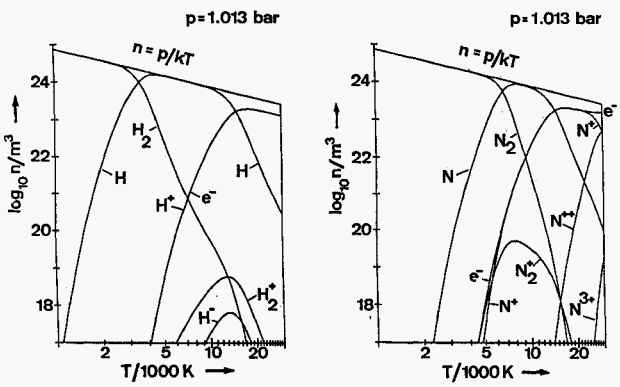


Fig. 3 Number density diagrams for $H_2$ and $N_2$ up to 30 000 K at atmospheric pressure /4/.

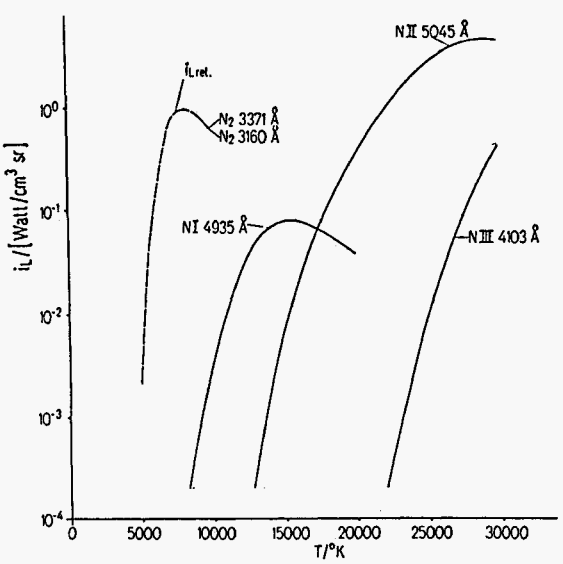


Fig. 4 Intensities of several spectral lines as function of temperature for $N_2$ (p = 1 bar) /3/.

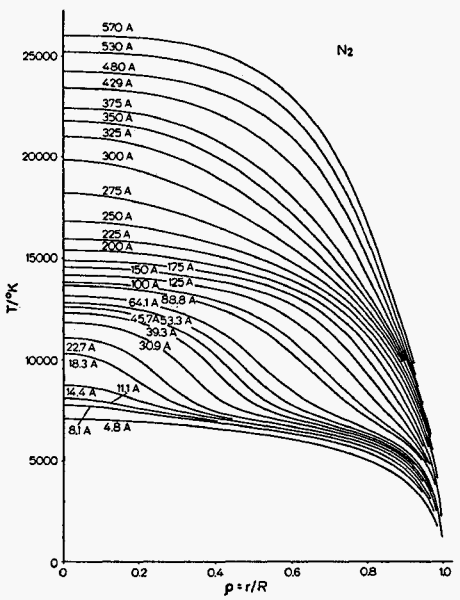


Fig. 5 Measured radial temperature distributions for various currents in $N_2$-arcs /3/.

This formula is essentially a product of two temperature functions, i.e. $n(T,p,)$ and $\exp(-E_m/kT)$. The dependence of the line intensity $I_l(T)$ on temperature (Fig. 4) is first governed by the steep increase of the exponential function and additionally (apart from the molecules) by the rise of the special number density with temperature. Thus, the absolute line intensity $I_L$ is a sensitive gauge for measuring plasma temperatures in those regions where the line intensities grow. With increasing temperatures the exponential function approaches unity and the number density of the respective particles decreases rapidly due to further ionizations. Therefore, the line intensity reaches a maximum and subsequently drops. The maximum of the line intensity is called the Larenz maximum and the related temperature the norm temperature /5/. So, wherever an intensity maximum is observed, whether visually or by spectral analysis there the related norm temperature can be attributed (e.g. Fig.2). The Larenz maximum is a valuable diagnostic tool for two reasons. Once an intensity maximum is found the temperature distribution on either side of the maximum can be determined without the difficulty of absolute measurements. Furthermore, on the base of the Larenz maximum an absolute radiation standard is available, making use of the high plasma temperatures. Therefore, it is most suitable for the uv and vuv spectral regions. This method is e.g. employed by the National Bureau of Standards in USA (NBS) /1/ using a hydrogen cascade arc observed end-on. The current is adjusted such that the maximum intensity of the chosen part of the spectrum, e.g. the Balmer continuum (370 nm > $\lambda$ > 125 nm) appears on axis. Then, the observed intensity equals the calculated maximum intensity which, particularly in the case of hydrogen, is precisely predictable (tube i.d. 2 mm; current about 80 A; $T_{norm}$ ca. 20 000 K depending on wave length $\lambda$ ). In this way, reactions such as dissociation or ionization provide valuable tools for spectral measurements by means of the Larenz maximum at the norm temperature. As an example for spectroscopic temperature measurements, the radial temperature distributions for various currents in cascade arc chambers are shown in Fig. 5.

## 3 REACTION HEAT CONDUCTION

The physical behaviour of a stationary arc is controlled by the energy equation, which means that the power supplied by Ohmic heating $\vec{j}\cdot\vec{E}$ has to be carried away by heat conduction $\vec{w} = -\varkappa \operatorname{grad} T$ and by radiation u

$$\vec{j}\cdot\vec{E} + \operatorname{div}(\varkappa \operatorname{grad} T) - u = 0 \tag{5}$$

(here the current density is $\vec{j} = \sigma(T)\vec{E}$ and the heat conductivity $\varkappa = \varkappa(T)$). Radiation losses u will not be considered in the following. After having chosen a parameter like the electrical field strength E, or the current I, or the power L per unit arc length the energy equation for the special case of cylindrical symmetry (Elenbaas-Heller)

$$\sigma\cdot E^2 + \frac{1}{r}\frac{d}{dr}\left(\varkappa r \frac{dT}{dr}\right) = 0 \tag{6}$$

yields the radial temperature distribution $T(r,I)$. Of course the material functions $\sigma(T)$ and $\varkappa(T)$ must be known. Normally, a bell shaped radial distribution results. Reaction zones, however, behave differently. Growing temperatures are correlated with an increase in the degree of reaction, resulting in additional particle gradients, namely of reaction products in the direction of higher temperatures and of original particles in opposite direction. These gradients cause the diffusion flows $\vec{J}_i = \varrho_i\vec{v}_i$ which can exist in steady state due to the continuing separation of reaction partners diffusing inwards to higher temperatures and to the recombination of separated partners diffusing outwards. The net mass flow through a test area must vanish due to steady state reasons

$$\vec{J}_1 + \vec{J}_2 = 0 \qquad \text{or} \qquad \vec{J}_2 = -\vec{J}_1 \tag{7}$$

The mass flows themselves, as expressed by the gradient of the particular mass concentration $c_1=\varrho_1/\varrho$ are

$$\vec{J}_1 = -\vec{J}_2 = -\varrho D_{12}\cdot\operatorname{grad} c_1 = -\varrho D_{12}\cdot(dc_1/dT)\cdot\operatorname{grad} T \tag{8}$$

with the usual definition of the diffusion coefficient D. The concentration gradient can be directly related to the temperature gradient, as already done in the above formula, by means of the number density diagrams in Fig.3. In contrast to the vanishing net mass flow, there exists a strong energy flow in the reaction zone, since the separated partners carry essentially the separation energy outwards and deposit it during recombination. This is the reason for a heat flow

$$\vec{w}_D = \vec{J}_1 h_1 + \vec{J}_2 h_2 = \vec{J}_1(h_1 - h_2) = -(h_1 - h_2)\cdot\varrho\cdot D_{12}\cdot(dc_1/dT)\cdot\operatorname{grad} T \tag{9}$$

where the difference of enthalpies per unit mass is the net dissociation energy of a molecule

$$h_1 - h_2 = -\frac{1}{m_1}\left(\frac{5}{2}kT + 2U_2 - U_1 + E_D\right) \tag{10}$$

Here, for a binary reaction, $2m_2=m_1$ has been used. $U_1$ and $U_2$ are the excitation energies per particle, respectively. In this way, a new, very effective heat conductivity in reaction zones has been introduced by

$$\varkappa_D = (h_1 - h_2)\,\varrho\, D_{12}\, dc_1/dT \tag{11}$$

In the case of ionization pairs of carriers bound by electric forces are produced diffusing together

against the diffusion flow of atoms and against the temperature gradient. This ambipolar diffusion results in the ionization heat conductivity

$$\varkappa_I = -\frac{1}{m_a}\left(\frac{5}{2}kT + U_i - U_a + E_I\right)\varrho\, D_{amb}\, d(\varrho_a/\varrho)/dT \qquad (12)$$

which again is much higher than the classical one. As an example, Fig. 6 shows the total heat conductivities of $H_2$ and $N_2$ both calculated and measured. In both cases the maxima in the dissociation and ionization regimes are distinctly marked.

In order to learn how the maxima of the heat conductivity $\varkappa_R$ in the reaction zones affect the performance of the arc, let us ask for the radial temperature distribution in the vicinity of the arc axis. For this purpose we approximate the T(r)-curve in the arc centre by a parabola

$$T(r) = T_A - \frac{1}{b}r^2 = T_A + \frac{1}{2}(d^2T/dr^2)_A\, r^2 + \ldots \qquad (13)$$

and compare this ansatz with the respective Taylor expansion.This procedure shows that the coefficient

$$b = -2\,(d^2T/dr^2)_A^{-1} = 2/k_A = 2\,R_A = d_A \qquad (14)$$

is identical with the diameter $d_A$ of the circle of curvature in the vertex of the downwards open parabola. So the coefficient b is a measure for the width of the arc core, which can be calculated from the cylindrical energy equation to yield

$$b = 4\,\varkappa_A/\sigma_A E^2 \qquad (15)$$

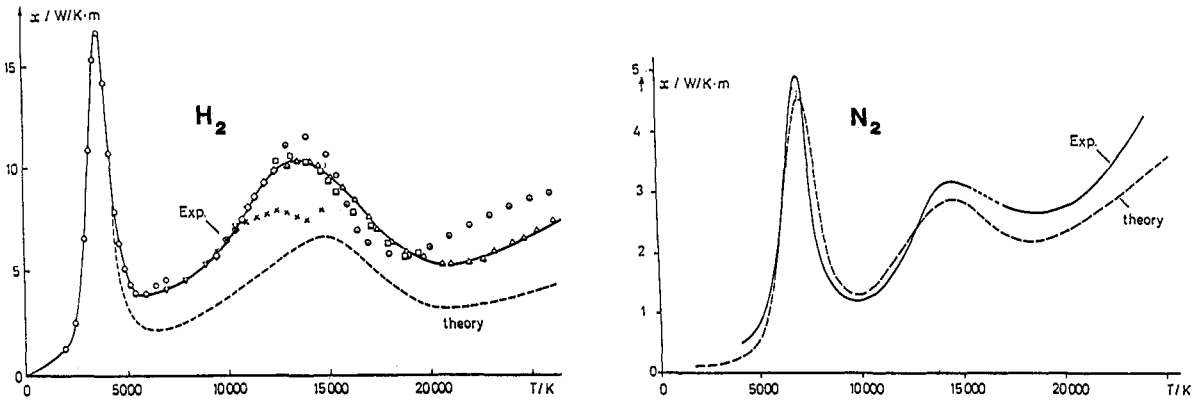


Fig. 6 Heat conductivities as function of temperature for $H_2$ and $N_2$. Notice in both curves the peaks in the dissociation and ionization regimes /6,7/.

Since the axial ohmic heating $\sigma_A \cdot E^2$ is a slowly varying function of I, the arc core will be broad for a high axial heat conductivity $\varkappa_A$ and narrow for low axial heat conductivities.

Now, after the breadth of the arc core let us investigate the axial temperatures in reaction zones. Here, the energy equation must be integrated twice in order to get the temperature itself. This can be done approximately by choosing a proper step function for the necessary material function, i.e. the electrical conductivity $\sigma(S)$ as a funtion of the heat flux potential S, defined by $dS = \varkappa dT$. The calculation yields for the increase of the axial temperature $T_A$ with Ohmic power L per unit arc length

$$\frac{dT_A}{dL} = \frac{1}{4\pi\varkappa_A} \quad \text{or} \quad dT = \frac{1}{4\pi\varkappa_A}\,dL \qquad (16)$$

where the increase of power dL can be performed by raising the current as well. The formula above can be best interpreted by saying that for constant increments of power dL the axial temperatures $T_A$ are the closer together the higher the heat conductivity $\varkappa_A$ is and vice versa. Thus, in the middle of the reaction zones where the heat conductivity $\varkappa_R$ is highest (Fig.7) a

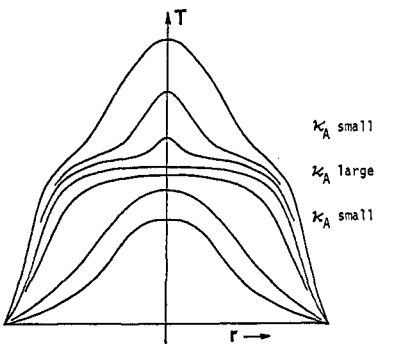


Fig. 7 Radial temperature distributions (schematic). Flat and close curves for high heat conductivities in the reaction regimes, small and distant curves in the minima of the heat conductivity.

set of closely spaced axial temperatures $T_A$ and very broad temperature distributions result while in the minimum beyond the reaction zone there appears a new narrow core with rapidly increasing axial temperatures when increasing the power or current. Exactly, this behaviour can be recognized at the radial temperature distributions of $N_2$ in Fig.5 at about 7000 K and higher for dissociation, and at about 14 000 K and higher for ionization.

The formation of an arc core beyond the dissociation regime can be observed very impressively in a free burning arc in air between a thin carbon cathode and a massive carbon anode at 200 A (Fig. 8). This so-called Beck arc or high intensity arc has a bright core in the centre which is caused by the minimum of the heat conductivity at about 10 000 K beyond the dissociation maximum of the reaction $N_2$ = 2N. The latter maximum is responsible for the flat temperature shoulders of about 7000 K around the core. Low current arcs do not show a core and operate only in the molecule region at very low degrees of ionization. Arcs in rare gases do not have a pronounced core either.

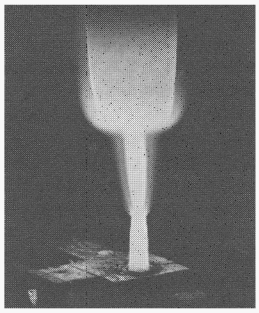

Fig. 8 High intensity arc in air at 200 A. Notice the white core emitted from atoms, the (blue-violet) aureol emitted from molecules, and the (yellow) border emitted from impurities /8/.

The high intensity arc exhibits an extraordinary stability due to selfmagnetic pinch forces driving the air along the cathode through the column towards the anode. The plasma jet produced in this way (200 m/s) stabilizes the arc and the gas flow from outside below is a substitute for constricting walls which would be necessary without flow. Finally, it should be emphasized that the cold gas flowing into the arc from below penetrates the dark dissociation zone without increasing its temperature very much, but gaining much enthalpy in form of dissociation energy. So, when hitting the anode, the plasma jet delivers a lot of energy to the anode and heats it up to high brightness. Similar processes occur in arc heating of work pieces, in welding, melting etc.

## 4 DEMIXING IN REACTION ZONES

Let us begin with a mixture of two gases, the one being an inert filling gas (subscript F), the other being able to undergo dissociations like $A_1=2A_2$. The mixing ratio may be described by the relative partial pressures at low temperatures $p_F/p=q$ and $p_{1_0}/p=1-q$. If now the temperature is raised at constant pressure p the degree of dissociation $x=p_2/(2p_1+p_2)$ increases likewise and the partial pressure of the molecules $p_1$ is being gradually replaced by that of atoms (Fig. 9). After completion of the dissociation the number of particles of the reacting gas has doubled while that of the inert gas is conserved. Regarding the total pressure p to be constant the relative partial pressure of the inert gas reduces from q to q/(2-q) and that of the reacting gas increases from 1-q to (1-q)/(1-q/2). Take e.g. q=1/2, then $p_F$ decreases from 1/2 to 1/3 and the reacting gas from 1/2 to 2/3. In the temperature gradient of an arc this means a creation of a partial pressure gradient for an inert filling gas in reaction zones directed outwards. This in turn causes a diffusion flow of the filling gas inwards according to

$$\vec{J}_F = -\rho \cdot D \cdot \text{grad}\, p_F \qquad (17)$$

which means the beginning of the demixing process and the enriching of the filling gas at higher temperatures. The final steady state is reached when no forces are acting on the filling gas i.e. when the filling gas does not have a partial pressure gradient anymore. For this approximation it is assumed that the opposing diffusion flows of the reactive partner do not exert a net friction force on the filling gas. If we permit a certain generalisation of the above considerations we may state that the gases with higher reaction energy are driven to higher temperatures and the more easily reacting gases outwards /9,10/.

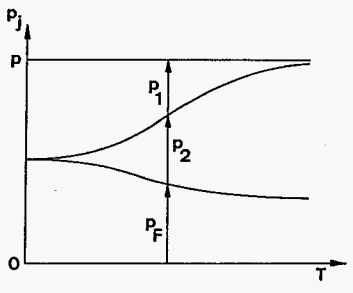


Fig. 9 Demixing in reaction zones (schematic). The reaction creates a gradient of the filling gas pressure.

The demixing processes occur in dissociation and ionization regimes likewise. In the above discussed example for dissociation one has to replace, in case of ionization, the number density of atoms by that of the charge carriers i.e. the sum of the ambipolar diffusing ions and electrons. The mass separation in arcs is of importance for quantitative spectroscopic measurements because one must not rely on the assumption that a gas mixture chosen for any investigation will be met again with the same ratio in the observations. For mass separation in large scale, the described process has not achieved any importance yet in spite of several trials.

## 5 CATAPHORESIS

Let us assume a cylindrical arc column without any dependence on the axial coordinate. In the partially ionized arc gas the electrons carry most of the current along the axis through the arc towards the anode driven by the axial electric field. The same field also drives the ions towards the cathode and no force stops this motion due to the cylindrical symmetry. Now the question arises, where the ions remain, after having reached the cathode. The answer is as follows: the ions recombine to neutrals by catching an electron from the cathode and form with time a fan like pressure gradient in front of the cathode until so many neutrals leave the cathode space as ions from the column reach the cathode. The neutrals travel back along the tube wall to the anode region. The pressure gradient at the cathode necessary for this circulating flow can be very small and cannot retard the ions in the column perceptibly. Particularily in free arcs or in wallstabilized arcs with a bypass connection between the anode and cathode space the equilization flow can run without any effect on the columns.

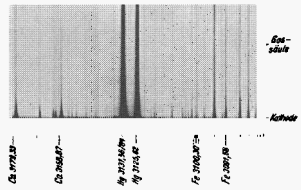

Fig. 10 Spectrum of the cathode region of a low current carbon arc showing the enrichment of added impurities /11/.

If now an easily ionizable trace gas is added to the arc it will almost completely be ionized and its ions will gather in front of the cathode and neutralize. Thereby a concentration gradient is formed which causes the trace gas to drift away by diffusion. This way an accumulation of the trace gas in front of the cathode is established which can be ten or a hundred fold the concentration in the column. This accumulation is of course the higher the more easily the trace gas can be ionized i.e. the lower the ionization energy is (Fig. 10). This process called cataphoresis is of importance for the proof of trace elements in the spectral analysis.

## 6 SUMMARY

In constricted arcs with axial temperatures of several ten thousand degrees, radial temperature gradients appear along which steady reactions i.e. either dissociations or ionizations occur. So the particle number densities grow and fall. Especially the spectral line intensities show up the so-called Larenz-maximum which is a valuable support for plasma diagnostics and temperature measurements.

In reaction zones a transport of reaction energy by diffusion takes place contributing to the heat conduction and being many times stronger than the classical heat conduction. The effect of the high heat conductivity in reaction zones of arcs is a distinct broadening of the arc and an only slow increase of the axial temperature with elevating power. But beyond the reaction zones at low heat conductivities again a fast rising arc core on the flat shoulders rises.

If the arc gas exists of a real mixture then a demixing process in reaction zones occur such that the component more difficultly to be dissociated or ionized gather at higher temperatures and the component more easily to be separated is pushed outwards.- Also the electric field effects a separation of species in axial direction in the sense that trace elements are collected in front of the cathode and that the more the lower the ionization potential is.

**Acknowledgements**

This paper is dedicated to Rudolf Wienecke on the occasion of his 65th birthday.

## REFERENCES

1. W.R. Ott, K. Behringer, and G. Gieres, Appl.Opt. 14, 2121 (1975).
2. S. Steinberger, Z. Physik 223, 1 (1969).
3. E. Schade, Z. Physik 233, 53 (1970).
4. W. Frie, personal communication.
5. R. W. Larenz, Z. Physik 129, 327, 343 (1951).
6. K. Behringer and Nguyen van Cung, Appl. Phys. 22, 373 (1980).
7. W. Hermann and E. Schade, Z. Physik 233, 333 (1970).
8. Courtesy R. Wienecke
9. W. Frie and H. Maecker, Z. Physik 162, 69 (1961).
10. J. Richter, Z. Astrophysik 53, 262 (1961).
11. R. Mannkopff, Z. Physik 76, 396 (1932).